Materials Science-Poland, Vol. 25, No. 4, 2007

Nanotribological characteristics of lanthanum-based thin films on phosphorylated 3-aminopropyltriethoxysilane self-assembled monolayers

G. QINLIN[1], X. CHENG[1,2*]

[1]School of Mechanical and Power Engineering, Shanghai Jiao Tong University, 200030, Shanghai, PR. China

[2]National Engineering Research Center for Nanotechnology, 200237, Shanghai, PR. China

Lanthanum-based thin films deposited on phosphonate 3-aminopropyltriethoxysilane (APTES) self-assembled monolayers (SAM) were prepared on a hydroxylated silicon substrate by a self-assembling process from a specially formulated solution. Chemical compositions of the films and chemical states of the elements were detected by X-ray photoelectron spectrometry. The thicknesses of the films was determined with an ellipsometer, while their morphologies and nanotribological properties were analyzed by means of atomic force microscopy. It was found that the lanthanum-based thin films showed the lowest friction and adhesion followed by APTES-SAM and phosphorylated APTES-SAM, while silicon substrate showed high friction and adhesion. Microscale scratch/wear studies clearly showed that lanthanum-based thin films were much more scratch/wear resistant than the other samples. The superior friction reduction and scratch/wear resistance of lanthanum-based thin films may be attributed to low work of adhesion of non-polar terminal groups and the strong bonding strength between the films and the substrate.

Key words: *lanthanum-based thin films; friction; adhesion; scratch; wear*

1. Introduction

Microelectromechanical systems (MEMS) and emerging nanoelectromechanical systems (NEMS) are expected to have a major impact on our lives, much like the way the integrated circuit has affected information technology [1, 2]. However, due to the large surface area to volume ratios in MEMS/NEMS devices as the size scale shrinks, many potential applications for MEMS/NEMS are not really practical at present. For

*Corresponding author, e-mail: xhcheng@sjtu.edu.cn

example, many studies have revealed a profound negative influence of stiction, friction and wear on the efficiency, power output, and steady-state speed of micro/nanodynamic devices [3–6]. Self-assembled monolayers (SAM) have gained growing interest over the past years because they have advantageous characteristics of well-defined structures, strong head group-substrate binding and dense packing of hydrocarbon chains. Indeed SAM considerably reduces friction and adhesion, and found use in various microelectromechanical systems (MEMS) devices [7–11].

Rare earths have been applied as important materials in high mechanical strength and fracture toughness applications, owing to their superior properties such as good friction-reducing, wear-resistant properties, excellent corrosion resistance and high anti-scuffing ability [12–16]. A number of studies have been done on the nanotribological properties of various SAMs [17, 18] but the study of the rare earth films on the nanotribological behaviour is still much lacking. In this study, lanthanum-based thin films deposited on the phosphorylated 3-aminopropyltriethoxysilane (APTES) SAM were prepared on silicon substrates. Several methods, such as X-ray photoelectron spectroscopy (XPS), atomic force microscopy (AFM), ellipsometer and contact angle measurements were applied to investigate the structure and nanotribological properties of the films.

2. Experimental

Preparation of lanthanum-based thin films on the phosphorylated APTES-SAM. 3-Aminopropyltriethoxysilane was purchased from Aldich Chemical Company, Inc. A single-crystal silicon wafer polished on one side was used as a substrate for the SAM transfer. Other reagents were of analytical grade. Deionized water was used throughout the experiment. For the preparation of the target solution, APTES, toluene, ethanol, acetonitrile, phosphorus oxychloride, and collidine were commercially obtained and used without further purification. The silicon substrates were cleaned with 'piranha' solution (H_2SO_4:H_2O_2=7:3 (v:v)), then exposed to a solution of APTES in toluene (2% V:V, 24h, room temperature), followed by $POCl_3$ in acetonitrile (0.2 M $POCl_3$, 0.2 M collidine, 20 min, room temperature) [19, 20]. This treatment resulted in the surface rich in phosphonate groups ($–PO(OH)_2$) which adsorbed a layer of lanthanum-based thin films when immersed in pre-prepared solution with $LaCl_3$, ethylenediamine tetraacetic acid (EDTA) etc. for 24 h, then cleaned ultrasonically with deionized water to remove other physisorbed ions or molecules and dried for 2 h at 120 °C, then naturally cooled in a desiccator. A schematic of growth of lanthanum-based thin films on phosphorylated APTES-SAM is shown in Fig. 1.

Apparatus and test procedures. Chemical compositions of the films and chemical state of the elements were analyzed with a PHI-5702 XPS system, using MgK_α radiation operating at 250 W and pass energy of 29.35 eV. The binding energy of C 1s (284.6 eV) was used as the reference. The resolution for the measurement of the bind-

ing energy is about ±0.3 eV. The static contact angles were measured in ambient air (relative humidity 40%) using an OCA-20 contact angle measurement device (Data-Physics Instruments Gmbh). Distilled water was used as the spreading reagent. Measurements were performed on at least three samples, and were made at a minimum of three different spots on each sample. The contact angles were typically reproducible to within ±2°. The thicknesses of the films were measured with an ellipsometer (V-VASE with AutoRetarder from J.A. Woollam Co., polarizer-retarder-sample-rotating analyzer configuration) which was equipped with a He-Ne laser (632.8 nm) set an incident angle of 70°. The index of refraction for the refraction was taken to be 1.45. Thickness data were obtained by averaging five measurements at different spots of each sample surface. The thickness was recorded with the accuracy of ±0.3 nm.

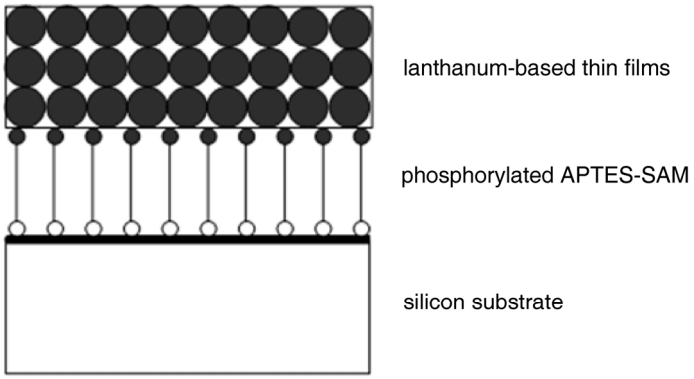

Fig. 1. Schematic of growth of lanthanum-based thin films on phosphorylated APTES-SAM

The surface morphologies and nanotribological properties of the films were investigated using an SPM-9500 atomic force microscope (NanoScope IIIa) produced by Shimadzu Corporation (Kyoto, Japan). Square pyramidal Si_3N_4 tips with the nominal 50 nm radius mounted on gold-coated triangular Si_3N_4 cantilevers with spring constants of 0.6 N/m were used. The adhesion and friction data were measured ten times at each interesting location and average data values were obtained. Adhesive forces were measured using the so called "force calibration plot" [18]. Friction forces were also measured according to Ref. [21]. By following the friction force calibration procedures developed by Bhushan [22], voltages corresponding to friction forces can be converted to force units. The coefficient of friction was obtained from the slope of friction force data measured as a function of normal loads.

For the scratch and wear tests, specially fabricated microtips were used. These microtips consisted of single-crystal natural diamond, ground to the shape of a three-sided pyramid, with an apex angle of 80° and tip radius of about 50 nm, mounted on a platinum-coated stainless steel cantilever beam whose stiffness was 50 N/m. Samples were scanned orthogonal to the long axis of the cantilever with loads ranging from 20 to 100 μN to generate scratch/wear marks. Observations of the sample surface

before and after the wear tests were done by scanning parallel to the long axis of the cantilever with loads ranging from 0.5 to 1 μN. The parallel scans enabled near-zero wear of the sample surface and also eliminated post-data analysis errors in surface feature height scratch/wear tests were performed over a scan area of 2×2 μm^2 at the scan rate of 10 Hz. The reported scratch/wear depths are an average of six runs at separate instances. In this study, all of the measurements were carried out in ambient conditions (22 ºC, RH 40–44%).

3. Results and discussion

3.1. Characterization of the prepared films

Figure 2 shows a series of AFM images taken over regions 1.0×1.0 μm^2 of specimens at various stages of the film deposition process, where a) refers to the bare cleaned silicon substrate, b) to APTES-SAM on the silicon substrates, c) to the phosphorylated APTES-SAM and d) to as-deposited lanthanum-based thin films on the phosphorylated APTES-SAM. It can be seen that the surface of the silicon substrates (Fig. 2a) is clean and smooth with surface root-mean-square (rms) roughness in the range of 0.2–0.3 nm. The surface in Fig. 2b is uniform and homogenous with surface rms roughness about 0.522 nm. The phosphorylated APTES-SAM (Fig. 2c) becomes more and more uniform and homogeneous with rms roughness about 0.393 nm. The possible reason is that the–$PO(OH)_2$ groups are bigger than the terminal groups –NH_2 which leads to the –$PO(OH)_2$ terminal molecules providing a more densely packed arrangement than the –NH_2 terminal molecules. After the deposition of the lanthanum-based thin films (Fig. 2d) on the phosphorylated APTES-SAM, many differences are visible in the corresponding AFM images. Namely, the surface of the as-deposited lanthanum-based films is rough and quite densely round-looking particles are visible with the rms roughness to be about 0.863 nm which shows wide potential application in lubrication and wear protection.

The XPS spectra applied to detect the chemical states of some typical elements for the prepared films are shown in Figs. 3–6. XPS survey and single scan spectra of APTES-SAM (Fig. 3) show contributions from the substrate and the film: silicon (15.5 at. %), carbon (56.3 at. %), oxygen (20.2 at. %), and nitrogen (8.0 at. %). Nitrogen is detected which indicates successful APTES-SAM deposition, since this element is only contained in this material.

Figure 4 shows single-scan XPS spectra of N 1s peak decomposed into two different nitrogen species occurring in various binding states. The peak at 400.8 eV is assigned to the protonated aliphatic amino groups, while that at 399.5 eV may be ascribed to the aliphatic amino groups. This interpretation is consistent with the data of Ref. [23]. After in situ phosphorylation of the APTES-SAM, the P 2p peak at 134.5 eV is observed (Fig. 5), which is assigned to the P atoms in –$PO(OH)_2$ group; N signal is absent. This indicates that the terminal –NH_2 group in the APTES-SAM has been phosphorylated and transformed to $PO(OH)_2$ group successfully and completely.

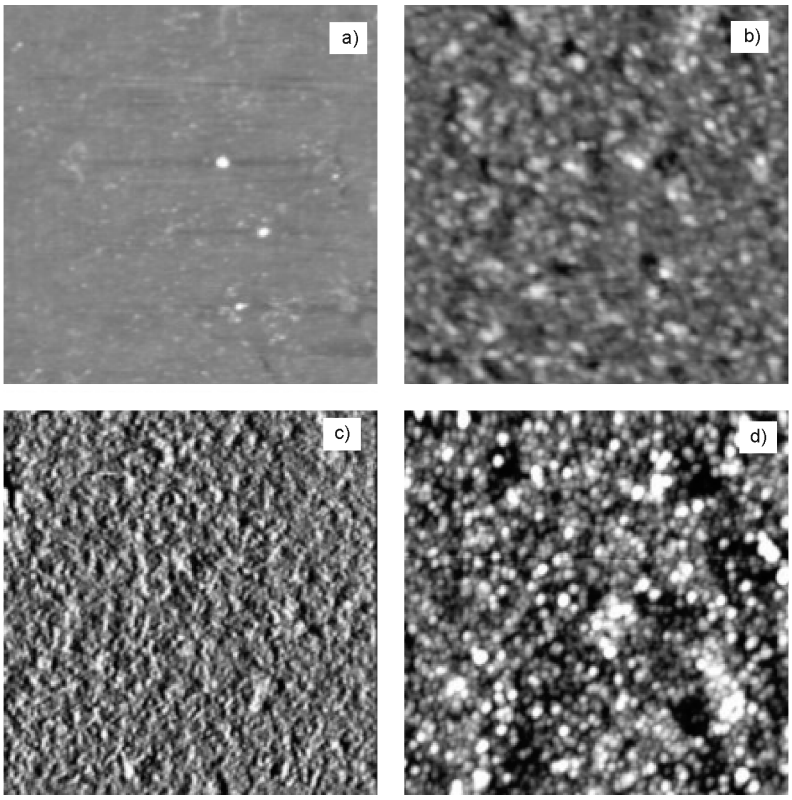

Fig. 2. AFM images of the surface of : a) bare cleaned silicon substrate, b) APTES-SAM on a silicon substrate, c) phosphorylated APTES-SAM, d) as-deposited lanthanum-based thin films on the phosphorylated APTES-SAM

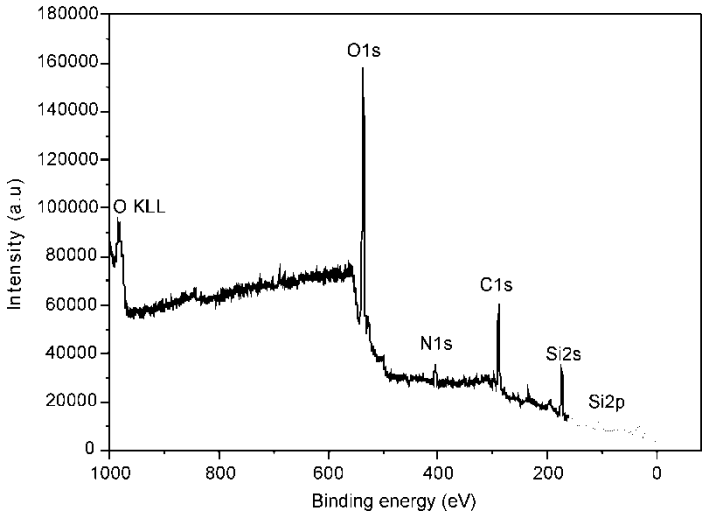

Fig. 3. XPS survey and single scan spectra of an APTES film

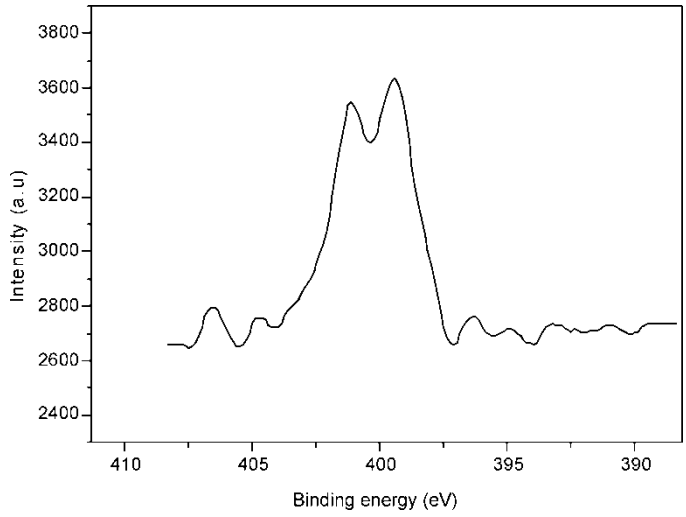

Fig. 4. Single scan XPS spectrum of the N 1s region of an APTMS film

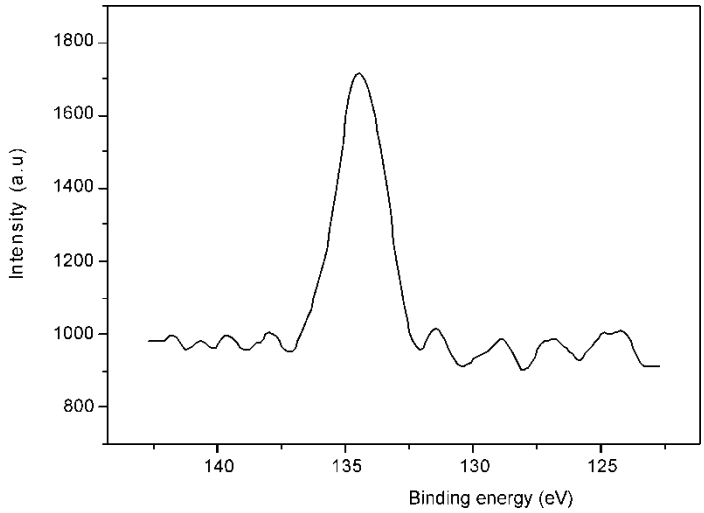

Fig. 5. Single scan XPS spectrum of the P 2p region in an APTMS film

Figure 6 shows a single-scan XPS spectrum of La 3d in the lanthanum-based thin films deposited on the phosphorylated APTES-SAM. The La^{3+} core level band of surface also decomposes into four peaks at binding energies of 835, 838.85, 851.725 and 855.225 eV, while the characteristic peak of La 3d in $LaCl_3$ (seen in Fig. 7) is at binding energies of 853.0 eV and 856.7 eV. As a result, a supposition can be made that lanthanum elements may react with $–PO(OH)_2$ group on the surface of substrate. The absence of Si signal indicates a complete coverage of the underlying silicon substrate by lanthanum elements.

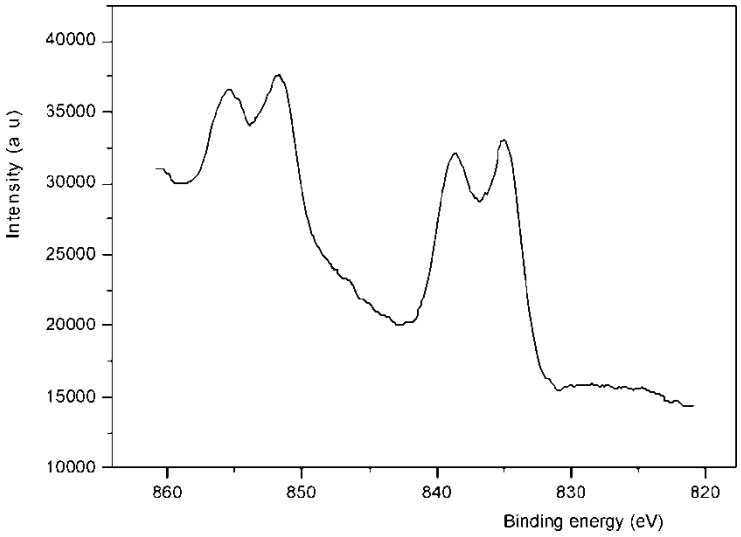

Fig. 6. XPS spectra of La_{3d} in an RE film

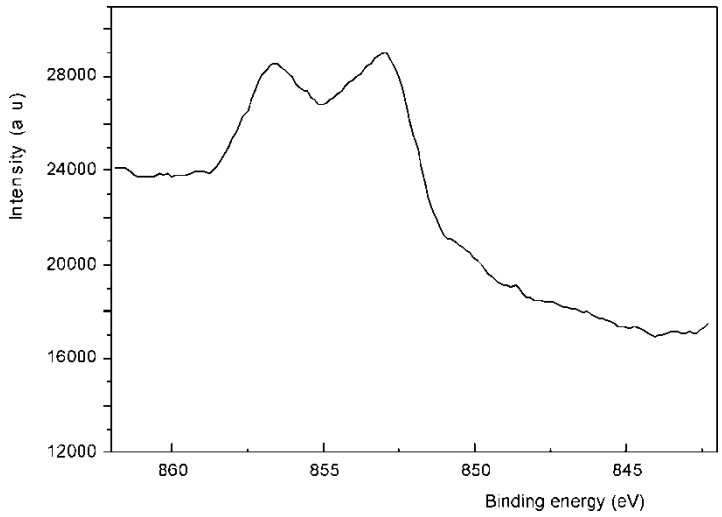

Fig. 7. XPS spectra of La_{3d} in $LaCl_3$

The contact angles of distilled water on the silicon substrate and on the prepared films have been measured. The APTES-SAM has a contact angle of 50º±2º, which is consistent with a moderately polar surface where the amino groups are oriented upward. After phosphorylation in situ for 20 min, a contact angle of 24º±2º is recorded for the phosphorylated surface. The contact angle of lanthanum-based thin films deposited on the phosphorylated APTES- SAM increases to 66º±2º.

In our work, the thicknesses of the prepared films on glass substrates were determined with an ellipsometer. The averaged thickness of the APTES-SAM is about

7.5 nm which matches with the projection of a normally extended molecular chain on the surface. The thickness is hardly changed after the $–NH_2$ is phosphorylated to $–PO(OH)_2$ group which indicates that a monolayer of phosphorylated APTES has been prepared on glass substrates. The thickness increases to ca. 15 nm after the phosphorylated APTES-SAM is immersed in the rare earth solution, which also shows that lanthanum-based thin films have been successfully obtained.

3.2. Nanotribological properties of the prepared films

Adhesion, friction and work of adhesion. Figure 8 shows the average values of the adhesion forces and coefficients of friction of four kinds of flat surfaces measured by contact mode AFM under an applied normal load of 20 nN and the scan rate of 10 Hz.

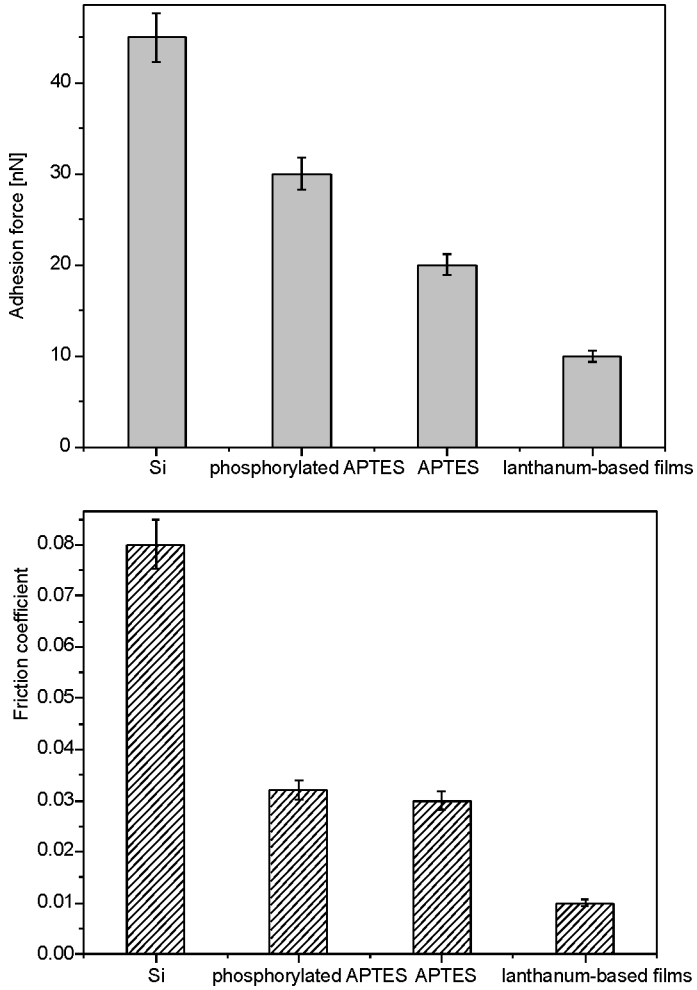

Fig. 8. Adhesive forces and coefficients of friction of silicon and prepared films

This shows that SAMs can reduce the adhesive and frictional forces of silicon substrate. In particular, lanthanum-based thin films exhibit the lowest adhesive force and coefficient of friction. This means that the prepared films can be used as effective molecular lubricants for micro/nanodevices fabricated from silicon. Based on the data, the ranking of adhesive forces F_a is in the following order: $F_{a\text{-Si}} > F_{a\text{-phosphorylated APTES}} > F_{a\text{-APTE}} > F_{a\text{-lanthanum-based films}}$, and the ranking of the coefficients of friction is in the following order: $\mu_{\text{Si}} > \mu_{\text{phosphorylated APTES}} \approx \mu_{\text{APTES}} > \mu_{\text{lanthanum- based films}}$.

Based on the Young–Dupre equation, the work of adhesion W_a

$$W_a = \gamma_{1a}(1 + \cos\theta_1) \tag{1}$$

required to pull apart the unit area of a solid interface [24] has been shown in Fig. 9. In Eq. (1), γ_{1a} is the surface tension of liquid–air interface and θ_1 is the contact angle

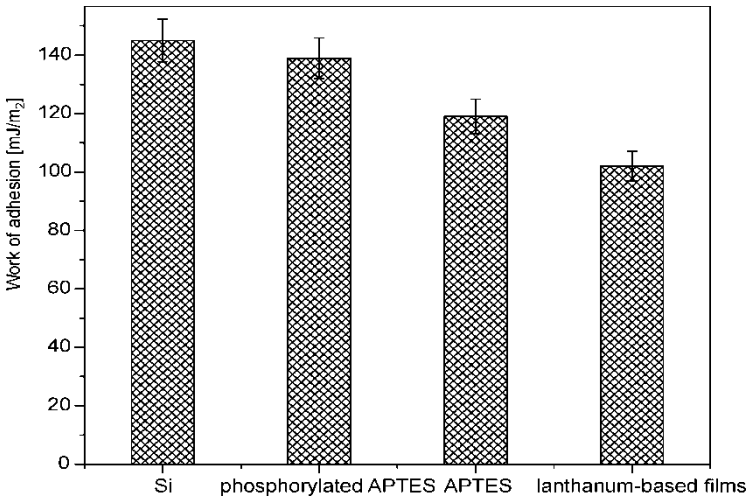

Fig. 9. Work of adhesion of silicon and prepared films

between water and a flat horizontal surface. From Figures 8 and 9 it was found that the adhesive force and friction coefficient decrease as the work of adhesion decreases. This implies that the capillary force acting between the tip and the flat surfaces seriously affects nano-adhesion and nano-friction. From Figure 8, it can also be found that APTES-SAM and phosphorylated APTES-SAM have polar surface groups ($–NH_2$ and $–PO(OH)_2$ groups), thus leading to larger W_a and eventually larger adhesive forces. The lanthanum-based films do not have polar surface groups, thus have a smaller W_a and adhesive force than APTES-SAM and phosphorylated APTES-SAM.

Scratch/wear tests. As explained earlier, the scratch tests of silicon and the prepared films were studied by making scratches (10 cycles per each load) with varying loads. Figure 10 shows the plot of scratch depth vs. normal load for various samples. Scratch depth increases with increasing normal load. APTES-SAM and phosphory-

lated APTES-SAM show similar scratch resistance. From the data, it is clear that the lanthanum-based thin films show the best scratch resistance compared with the silicon substrate, APTES-SAM and phosphorylated APTES-SAM. The increase in scratch depth with normal load is very small and all depths are less than 20 nm, while the silicon substrate and APTES-SAM finally reach depths of about 80 nm and 150 nm, respectively.

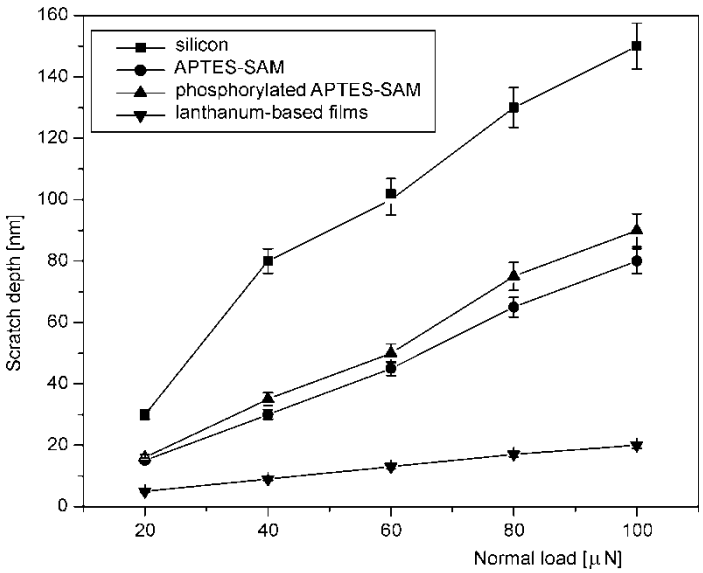

Fig. 10. Scratch depths for 10 cycles as a function of normal load

Wear tests were conducted on the samples by wearing the same region for 30 cycles at a normal load of 20 μN, while observing wear depths at different intervals (1, 5, 15, 20 and 30 cycles). This would give information on the progression of wear of the films. The observed wear depths are plotted against number of cycles in Fig. 11. For all samples, the wear depth increases almost linearly with increasing number of cycles. This suggests that material is removed layer by layer in all materials. Here also, lanthanum-based thin films exhibit a lesser increase in wear depth (lower slope) than the other samples. APTES-SAM wears less than the silicon substrate, which shows similar wear characteristics to the phosphorylated APTES-SAM. Combined with the scratch/wear data and the thickness of the films, it can be found that the scratch/wear depths of APTES-SAM and phosphorylated APTES-SAM are much larger than their thickness (7.5 nm). On the contrary, the scratch/wear depths of lanthanum-based thin films do not exceed their thickness (15 nm) all the time. It shows that APTES-SAM and phosphorylated APTES-SAM are seriously destroyed with the increase of normal load and number of cycles, while lanthanum-based thin films are still not completely worn. The scratch/wear results indicate that lanthanum-based thin films have better

surface mechanical properties than silicon substrate, APTES-SAM and phosphorylated APTES-SAM.

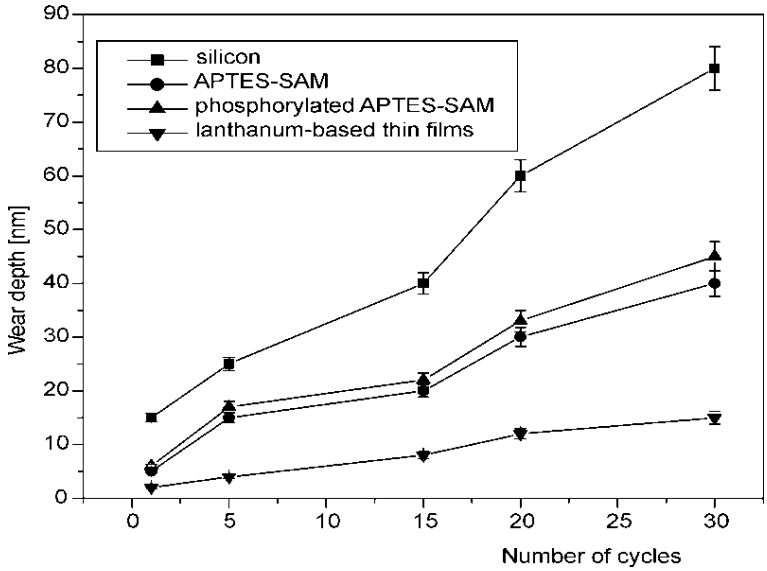

Fig. 11. Wear depths as a function of number of cycles

Rare earth elements have excellent chemical activity which results from their special 4f electron shell structure. Since electrons on the 4f electronic shell do not screen entirely the atomic nucleus, rare earth atom has a high effective nuclear charge [16, 25]. The $–PO(OH)_2$ group on the APTES-SAM provides net negative charge, thus promoting the process of self-assembly. First, La^{3+} ion is adsorbed on the negatively charged surface of phosphorylated APTES-SAM. Then $–PO(OH)_2$ group not only has proton to exchange with lanthanum cation but also can provide a P=O bond as complexing group to react with lanthanum elements after adsorption, thus improving the bonding strength between the films and the silicon substrates [26]. In addition, Hertzian cone cracks can occur when the normal stress exceeds a critical value as the AFM tip slides over the surface [27]. Friction forces during sliding reduce this critical value. In a word, strong bonding strength between the films and the silicon substrates and low coefficient of friction are responsible for the superior scratch/wear resistance of lanthanum-based thin films.

4. Conclusions

In this work, nanotribological properties of silicon substrate, APTES-SAM, phosphorylated APTES-SAM, and the lanthanum-based thin films were characterized by

an AFM. The lanthanum-based thin films showed the lowest friction and adhesion followed by APTES-SAM and phosphorylated APTES-SAM, while silicon substrate showed high friction and adhesion. Microscale scratch/wear studies clearly showed that lanthanum-based thin films were much more scratch/wear resistant than the other samples. The superior friction reduction and scratch/wear resistance of lanthanum-based thin films may be attributed to low work of adhesion of non-polar terminal groups and the strong bonding strength between the films and the substrate.

It is thus concluded the prepared lanthanum-based thin films could be used for protection from scratching as well as reducing friction.

Acknowledgements

Authors would like to thank for the National Natural Science Foundation of China (grant No. 50475023) and Instrumental Analysis Center, Shanghai Jiao Tong University support for the present work.

References

[1] *Microelectromechanical Systems: Advanced Materials and Fabrication Methods*, NMAB-483, National Academy Press, Washington, DC, 1977.
[2] ROUKES M., Phys. World, 14 (2001), 25.
[3] BHUSHAN B., *Tribology Issues and Opportunities in Mems*, Kluwer Academic, Dordrecht, 1998.
[4] BHUSHIAN B., *Handbook of Micro/Nanotribology*, 2nd Ed., CRC, Boca Raton, FL, 1999.
[5] KAYALI S., LAWTON R., SMITH B.H., IRWIN L.W., EEE Links, 5 (1999), 10.
[6] ARNEY S., MRS Bull., 26 (2001), 296.
[7] BHUSHAN B., ISRAELACHVILI J.N., LANDMANN U., Nature, 374 (1995), 607.
[8] DUGGER M.T., SENFT D.C., NELSO G.C., ACS Symp. Ser., 741 (2000), 455.
[9] DEPALMA V., TILLMAN N., Langmuir, 5 (1989), 868.
[10] TSUKRUK V.V., BLIZNYUK V.N., HAZEL J., VISSER D., EVERSON M.P., Langmuir, 12 (1996), 4840.
[11] BOSHUI C., YI Y., JUNXIU D., J. Chin. Rare Earth Soc., 16 (1998), 220.
[12] KONISHI Y., SHIMAOKA J.C., ASAI S., React. Funct. Polym., 36 (1998), 197.
[13] SIDEBOTTOM D.L., HRUSCHKA M.A., POTTER B.G., BROW R.K., J. Non-Cryst. Sol., 222 (1997), 282.
[14] CHENG X.H., BAI T., WU J., LIANG W., Wear, 260 (2006), 745.
[15] YU L.G., LIAN Y.F., XUE Q.J., Wear, 214 (1998), 151.
[16] CHENG X.H., C.Y.XIE, Wear, 254 (2003), 415.
[17] CHA K.H., KIM D.E., Wear, 251 (2001), 1169.
[18] BHUSHAN B., Wear, 259 (2005), 1507.
[19] BUSCHER T.C., MCBRANCH D., DEQUAN L., J. Am. Soc., 118 (1996), 2950.
[20] KATZ H.E., SCHELLER G., PUTVINSKI T.M., SCHILLING M.L., WILSON W.L., CHIDSEY C.E.D., Science, 254 (1991), 1485.
[21] BINNIG G., QUATE C.F., GERBER CH., Phys. Rev. Lett., 56(1986), 930.
[22] GLOSLI J.N., MCLELLAND G.M., Phys. Rev. Lett., 70 (1993), 1960.
[23] BIERBAUM K., KINZLER M., WÖLL CH., GRUZNE M., HÄHNER G., HEID S., EFFENBERGER F., Langmuir, 11 (1995), 512.
[24] ISRAELACHVILI J.N., *Intermolecular and Surface Forces*, Academic Press, New York, 1985.
[25] BELL T., SUN Y., LIN Z., YAN M., Heat Treat. Met., 27 (2000), 12.

[26] KANTIPULY C., KATRAGADDA S., CHOW A., Talanta, 37 (1990), 491.
[27] HUTCHINGS I.M., *Tribology, Friction and Wear of Engineering Materials*, CRC Press, Boca Raton, FL, 1992.

Received 10 July 2007
Revised 7 September 2007